Study of the Flexural Modulus of Natural Fiber/Polypropylene Composites by Injection Molding

Shinichi Shibata, Yong Cao, Isao Fukumoto

Department of Mechanical Systems Engineering Systems, University of the Ryukyus, Okinawa 903-0213, Japan

Received 4 May 2005; accepted 9 July 2005
DOI 10.1002/app.22609
Published online 11 January 2006 in Wiley InterScience (www.interscience.wiley.com).

ABSTRACT: Effect of fiber compression on flexural modulus of the natural fiber composites was examined. The kenaf, bagasse, and polypropylene were mixed into pellets, and composites were fabricated by injection molding. To predict flexural modulus of the composites, the Young's modulus of kenaf and bagasse fiber were measured. Using the obtained Young's modulus, the flexural modulus of the composites was predicted by Cox's model that incorporates the effect of fiber compression. It was found that those fibers with high Young's modulus were more compressed than that with low Young's modulus. Moreover, the distribution of fiber length and orientation in the composites were also investigated. To calculate the orientation factor for the prediction model, the distribution function of fiber orientation was determined to a triangular function. The flexural modulus of the composites increased with increase of volume fraction. The predicted values were in good agreement with the experimental values. Furthermore, it was revealed by SEM that the porous structure of the natural fibers was compressed. The fiber compression ratio (3.6) in bagasse was higher than that in kenaf (1.4) due to the difference in porous structure. © 2006 Wiley Periodicals, Inc. J Appl Polym Sci 100: 911–917, 2006

Key words: composites; polypropylene; injection molding; stiffness; reinforcement

INTRODUCTION

Recently many studies have been made to assess the use natural fibers as the reinforcement for composites. Kenaf,[1,2] jute,[3–7] ramie, oil palm,[8] hemp,[9,10] henequen,[11] and bagasse[12,13] composites were investigated in view of mechanical properties. The comparative analysis among those natural fibers has also been done.[14] These early reports revealed that the mechanical properties of these natural fiber composites have potential to replace traditional reinforcements like glass fiber due to economical and environmental reasons. In fact, a number of automotive components are fabricated using these natural fiber composites.

According to these many reports, there are very few studies about the prediction of the flexural modulus of natural fiber composites, though the prediction is essential for material design and fabrication of mechanical parts. Prediction of the flexural modulus of traditional short fiber-reinforced materials has been studied by Cox[15,16] and Fukuda et al.[17] using Young's modulus of matrix and fiber, and fiber orientation function. Moreover, Shibata et al.[18] have reported that the fiber compression should be incorporated into this prediction model because bagasse fiber has a porous structure in the cross section. However, the fiber compression in the injection molding process was not examined. Also, the compression of other fibers like kenaf, which is of interest in view of its high Young's modulus, was not revealed.

Thus, the objective of the present article is to predict the flexural modulus of natural fiber composites from polypropylene, kenaf, and bagasse in injection molding. The prediction using Cox's model[15,16] that incorporates the compression ratio of fibers was compared to the experimental result.

EXPERIMENTAL AND METHODS

Materials

Kenaf was supplied by Toyota Boshoku Co. Ltd., Japan. Kenaf fiber was straight and 70 mm length. The average fiber diameter was 0.094 mm.

Bagasse that had been obtained as the leftover after liquor extraction in a sugar mill was dried for 72 h at 80°C. The bagasse was sieved and the pith was removed. The average fiber diameter was 0.390 mm

Polypropylene (PP, Sumitomo Noblen AZ864N, molecular weight 2×10^5) as a matrix was received from Sumitomo Chemical Co., Ltd, Japan. The mechanical properties of these fibers and PP are shown in Table I. These properties were measured by the following experimental procedure.

Each fiber and PP were compounded with a kinetic pressure mixer, known as a double arm kneading mixer (type S5–2, Moriyama Co. Ltd., Japan) at 190°C

Correspondence to: S. Shibata (shibata@tec.u-ryukyu.ac.jp)

TABLE I
Mechanical Properties of Kenaf, Bagasse, and Polypropylene

	Young's modulus (MPa)	Tensile strength (MPa)	Specific gravity (kg/m^3)	Diameter (mm)
Kenaf	22,070	335	956	0.094
Bagasse	4,517	89	344	0.39
Polypropylene	1,315	24	902	—

for 1 h in air. Then, the compound was pulverized with the mixer for 6 h into pellets (2–5 mm in diameters) during cooling.

Figure 1 shows TGA results for kenaf and bagasse. The TGA curves were measured at 10°C/min for 6 mm each fibers in air with RIGAKU Thermo plus, TG8120, Japan. As shown in the figure, both fibers were rather stable below 190°C, and the weight loss rates in the temperature range 180–190°C were 0.1% and 0.05% per minute for kenaf and bagasse. From the results, the expected weight losses in the kneading process were 3% for kenaf and 6% for bagasse, respectively. These values were not extremely small, however, the effect of the thermal degradation on flexural modulus of composites was assumed to be small and negligible in this article.

The compounds were prepared at 10, 20, and 30% fiber weight fractions to investigate the effect of fiber volume on flexural modulus.

The pellets were molded into composites by a 10-ton injection-molder (type PS10E1ASE, Nissei Co. Ltd., Japan). The injection was carried out at a barrel temperature 165°C, a hold pressure 11 MPa, a mold temperature 90°C, a cooling time 7 s, a screw rotation speed 50 rev/min, and a injection speed 0.5 s/shot. The prepared composite was of cylindrical shape, 60 mm long, and having a diameter of 5.8 mm.

Measurement of Young's modulus and flexural modulus

To determine the Young's modulus of bagasse and kenaf fiber, each 72 fibers were tested. Span length and a cross head speed were 15 mm and 1 mm/min with a testing machine (type DCS-*R*-100, Shimadzu, Japan). Randomly chosen fibers were mounted on a paper tab with both ends of the fiber glued. The diameters were measured at three points of the fiber by an optical projector (Nikon, type V16-D, Japan), assuming that the fiber was a cylindrical.

Flexural test was carried out using a three-point flexural method (ISO 178) on five composites in each injection molding material (5.8 mm diameter). Span length and a cross-head speed were 55 mm and 1 mm/min.

Impact test and fractography observation

Impact test was performed to examine the fractography of composites at room temperature with Charpy impact tester (Ueshima Seishakusho, Japan). The capacity of impact testing machine was 0.3 kgf m. After the impact test, the fracture surface was coated with gold in vacuum. Then, the fractography was observed with SEM (Topcon, WS250, Japan) at 25 acceleration voltage.

Prediction of flexural modulus

It is well known[16] that Young's modulus of a short fiber-reinforced composite is determined by

$$E_{comp} = \eta_\theta \eta_f V_f E_f + (1 - V_f) E_m \tag{1}$$

where E_f , E_m, and V_f denote the Young's modulus of the fiber, the matrix, the volume fraction of the fiber in the composite. η_f , η_θ denote efficient factors of fiber length and orientation. η_f is given[11,12] by

$$\eta_f = 1 - \left(\tanh\frac{1}{2}\beta L\right)/\frac{1}{2}\beta L \tag{2}$$

$$\beta = \left(\frac{2G_m}{E_f r_f^2 \ln(R/r_f)}\right)^{\frac{1}{2}} \tag{3}$$

Equation 2 means the Young's modulus of the composite decreases with decreasing the fiber length l, where r_f and R denote the radius of the fiber and the interval among fibers. If the distribution of the fibers is homogeneous in an ideal packing square composite, R is given by

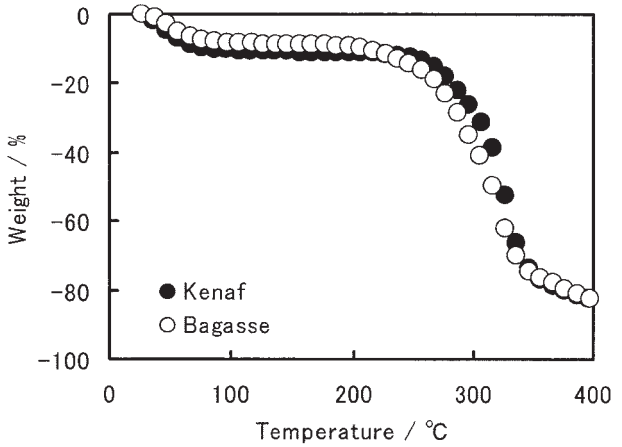

Figure 1 TGA curves of kenaf and bagasse as a function of weight loss and temperature.

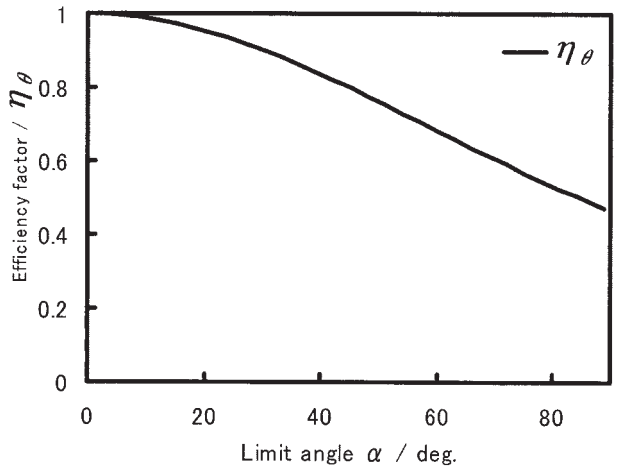

Figure 2 Relationship between orientation efficiency factor and limit angle.

$$R = \frac{r_f}{2}\sqrt{\frac{\pi}{V_f}} \tag{4}$$

Shear modulus G_m with assuming that the composite is an isotropy given by

$$G_m = \frac{E_m}{2(1 + v_m)} \tag{5}$$

where r_f and $\nu_{m;}$ denote the radius of the fiber and Poisson's ratio of the matrix that assumed ν_m is 0.3.

On the other hand, the efficiency factor η_θ has been analyzed by Fukuda et al.[17] using a probabilistic theory and assuming orientation distribution functions. The distribution functions are categorized by rectangular, sinusoidal, and triangular distribution, respectively. Judging from the experimental result as shown later in Figure 7, we assumed the triangular distribution as an orientation distribution function. This function is given by

$$g(\theta) = \begin{cases} -2\theta/\alpha^2 + 2/\alpha & (0 \le \theta \le \alpha) \\ 0 & (\alpha < \theta) \end{cases} \tag{6}$$

where α_0 denotes the limit angle of fiber orientation. If we experimentally determine the angle α, the orientation efficiency factor is given by

$$\eta_\theta = 4\frac{1 - \cos\alpha}{\alpha^2}\left(\frac{3 - v}{4}\cdot\frac{1 - \cos\alpha}{\alpha^2} + \frac{1 + v}{4}\cdot\frac{1 - \cos 3\alpha}{9\alpha^2}\right) \tag{7}$$

This distribution function assumes that the fiber distribution is two-dimensional. Figure 2 shows the relationship between η_θ and limit angle α. Efficiency factor η_θ is 1 at 0° (unidirectional fiber distribution), while it is 0.47 at 90°.

Finally, as described later [Figs. 5 (a,c)], the kenaf is like solid while bagasse is porous. Thus, the fiber compression in composites is expected to be quite different between bagasse and kenaf. Moreover, the authors assumed that when fibers are compressed, Young's modulus increases proportionally. The compression ratio is defined by the ratio of the original fiber volume to the fiber volume in the composite. Hence, the compression ratio, K, can be calculated by

$$K = V_f' \Big/ \left[V - \left(\frac{W - W_f}{\rho_m} \right) \right] \tag{8}$$

where V'_f, V, W, W_f and ρ_m denote original fiber volume, volume of the composite, weight of the composite, weight of the fiber, and density of the matrix, respectively. Therefore, the final equation that predicts flexural modulus of the composite is

$$E_{comp} = K\eta_\theta - \eta_f V_f E_f + (1 - V_f)E_m \tag{9}$$

RESULTS AND DISCUSSION

Young's modulus of kenaf and bagasse fiber

Figure 3 shows the relationship between Young's modulus and fiber diameters. Kenaf fibers were found to be higher in Young's modulus than bagasse fibers. Average Young's modulus of kenaf and bagasse were 22,070 MPa and 4517 MPa. These Young's modulus and fiber diameters were used for the prediction of flexural modulus by Equation 9.

The big scatter in Young's modulus may have relationship with the damages for fibers. However, Figure 4 shows the comparison of strong and weak fiber in the cross section for kenaf and bagasse after tensile test. It was clearly observed that in both fibers, the

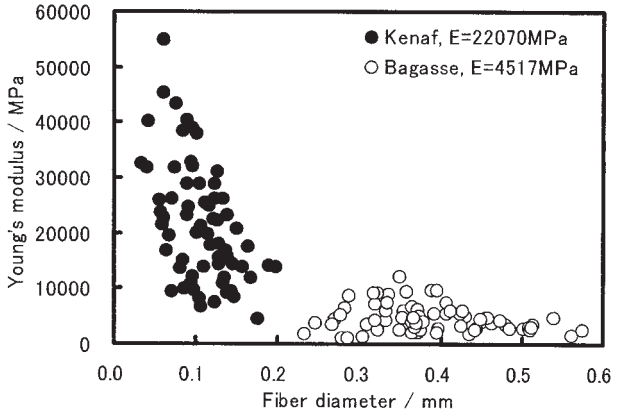

Figure 3 Relationship between Young's modulus and diameters of fibers.

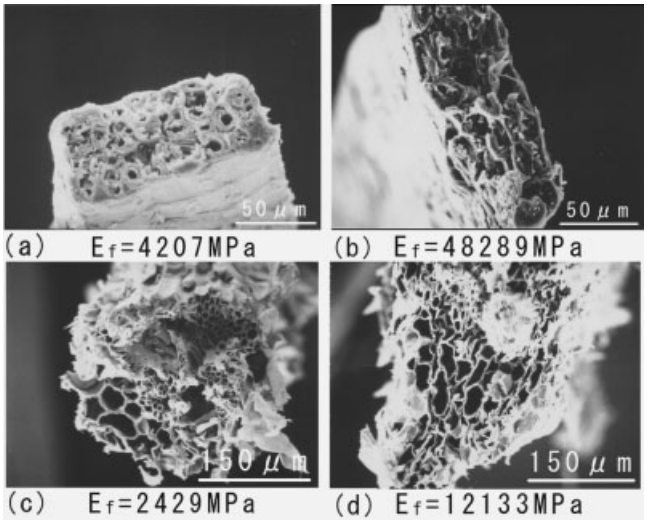

Figure 4 SEM photographs of the cross section of fibers after tensile test, (a) and (b) kenaf, (c) and (d) bagasse.

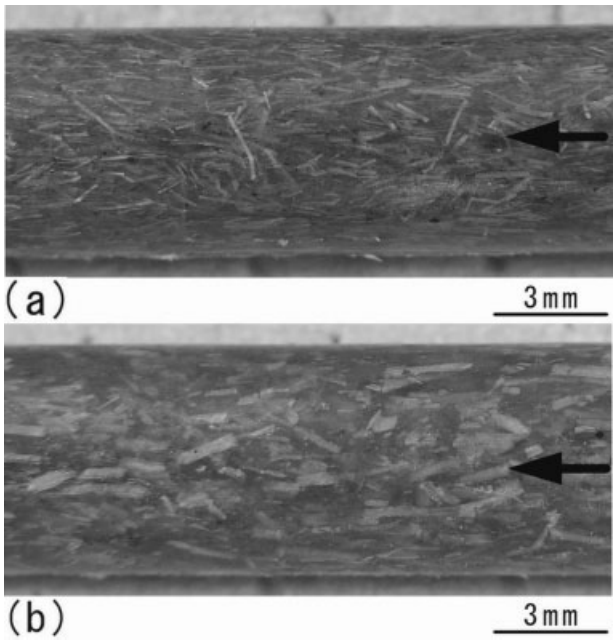

Figure 5 Optical microphotographs of injection molding composites, (a) kenaf (24 vol %) and (b) bagasse (26 vol %).

fiber with high Young's modulus was more compressed than that with low Young's modulus. In the case of high Young's modulus, each fibrous cell that had been circle in shape was deformed to elliptical because of large deformation. This deformation is considered to occur before the tensile test, because the elongation of each fiber in the photographs was quite small, (a) 1.27%, (b) 2.03%, (c) 1.68%, and (d) 2.38%. On the other hand, both kenaf and bagasse has been chopped mechanically, and some of fibers have been compressed before tensile test. These fibers were small in diameters because of the compressed structure. Hence, this compression is considered to make the fibrous structure dense and increase the Young's modulus of fiber.

This observation is in agreement with the results presented in Figure 3. In that figure, the fiber with small diameter has higher Young's modulus than that with large diameter.

Therefore, it is validated that the effect of fiber compression should be incorporated in the prediction model for the flexural modulus of natural fiber composites.

Fiber orientation and length of composites

Figure 5 shows the optical microphotographs of the composite by the injection molding. As shown in the figures, the fibers in the composites have certain orientation distribution, and most of fibers are oriented to the injection direction in both kenaf and bagasse. Moreover, it is clearly found that the diameter of kenaf is thinner than that of bagasse.

Figures 6 and 7 show the fiber length and orientation distribution on the surface of the composites. In each composite, 600 randomly chosen fibers were measured. Frequency on the y-axis of the figures means fiber existing possibility in the rage, which is 0.25 mm for fiber length and 10° for fiber orientation. Each number with SD in the figures is the standard deviation of data. The orientation angle was defined as the angle between the longitudinal axis of the composite and the axis of the fiber. As shown in Figure 6, in both fibers, the length distribution of fibers was similar, though the average fiber lengths for kenaf (1.34 mm) were longer than for bagasse (1.22 mm). This may be attributed to the same kneading and injection condition. Furthermore, in both fibers, the distribution of fiber orientation was similar also. The

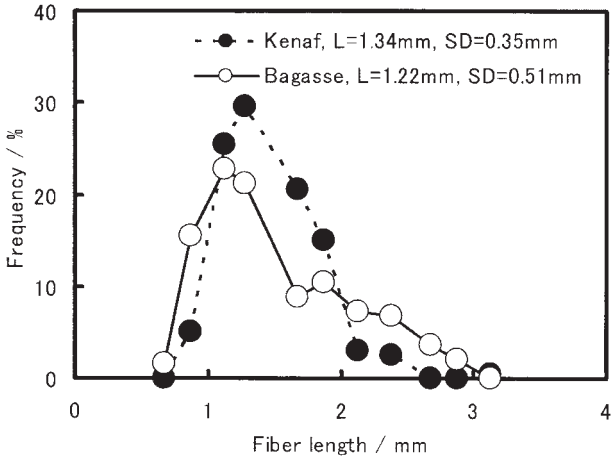

Figure 6 Distribution of fiber length of kenaf and bagasse composites.

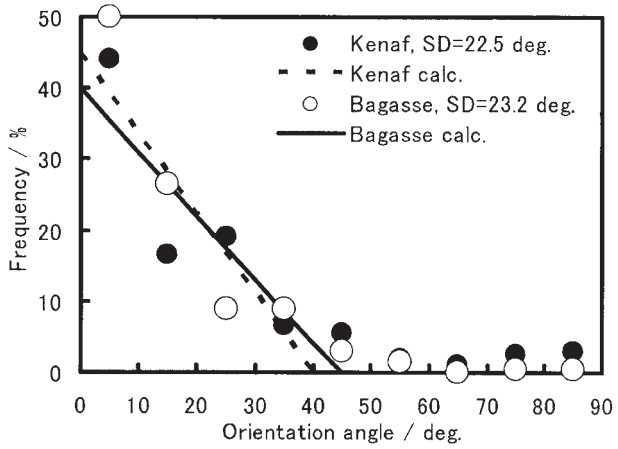

Figure 7 Distribution of fiber orientation angle of kenaf and bagasse composites.

limit angles α_{00} in eq. (6) were 40° and 45° for kenaf and bagasse. With these results, the orientation efficiency factor η_θ in eq. (7) by substituting α was calculated at 0.70 and 0.78 for kenaf and bagasse, respectively.

Figure 8 shows the optical microphotographs of the polished cross section parallel to the injection direction as indicated by arrows. The top and bottom of photographs are corresponding to the surface of the cylindrical composite. In the case of kenaf composite, the fiber distribution seemed to be homogeneous. On the other hand, the bagasse composite has longer fibers in the center than on the surface. In addition, the direction of some fibers in the center was not directed to the injection direction.

This could be an explanation why the bagasse fiber length was shorter than kenaf fiber length in Figure 6. This difference between kenaf and bagasse might be attributed to the difference flow in the mold. The detail is not clear at this point. This inhomogeneous fiber distribution in length and orientation would have certain effect on the flexural modulus. However, the flexural modulus is determined mostly by the fiber in the surface. Hence, this effect was considered to be small and neglected in this article.

Flexural modulus of the natural fiber composites

Figure 9 shows the relationship between flexural modulus and volume fraction of the fibers. According to the law of mixture, the flexural modulus increased with increasing the volume fraction of the fiber in both kenaf and bagasse. The transformation of the weight fraction into the volume fraction of the fibers was calculated by

$$V_f = \left[V - \left(\frac{W - W_f}{\rho_m} \right) \right] \Big/ V \qquad (10)$$

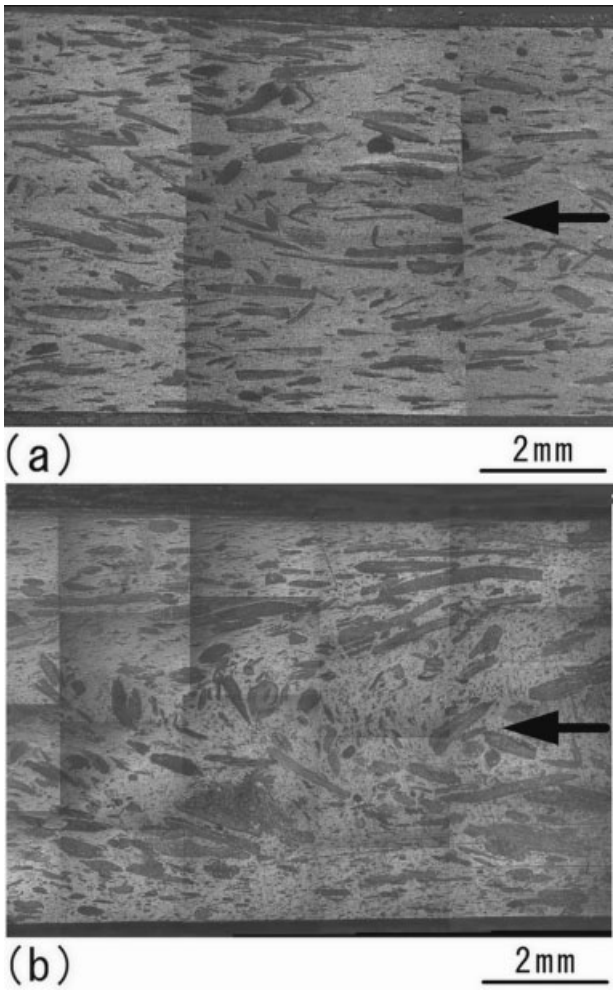

Figure 8 Optical microphotographs of the polished cross section parallel to the injection direction, (a) kenaf (24 vol %) and (b) bagasse (26 vol %).

where W_m, ρ_m, V, and V_f denote the matrix weight, the density of the matrix, the volume of the specimen, and the volume fraction of the fiber, respectively.

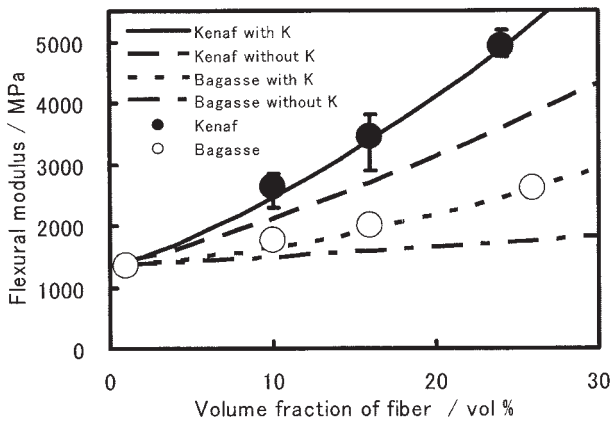

Figure 9 Relationship between flexural strength and volume fraction of composites.

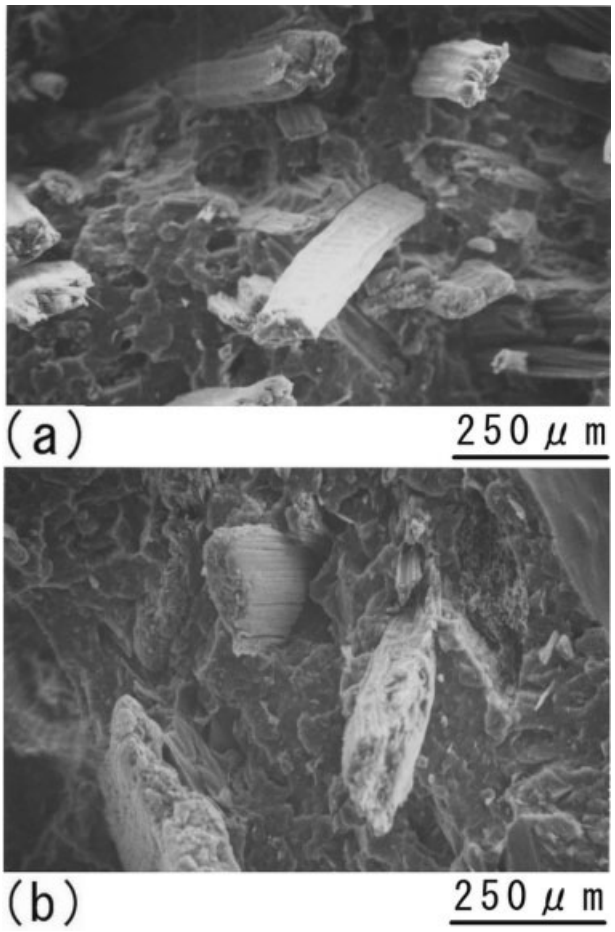

Figure 10 SEM microphotographs of the fracture surfaces of the composite after Charpy impact test, (a) kenaf (24 vol %) and (b) bagasse (26 vol %).

Figures 10(a) and 10(b) show SEM microphotographs of the fracture surface of the kenaf and bagasse composite after impact test. As shown in the figures, there were both pulled out fibers and broken out fibers. The pulled out fibers indicate the interfacial interaction was not so strong, while the interfacial interaction for broken fibers were so. Also, this difference should have relation with the critical length, which is difficult to identify. Thus, this issue is complicated and the authors hope to investigate the detail in future. Figures 11(a) and 11(b) show the cross sections of broken out fibers for kenaf and bagasse. To compare the structure as shown in Figure 4, the cross sections were clearly compressed.

These fiber compressions should occur somewhere from kneading process to injection molding. Hence, bagasse fiber samples was taken and observed after the kneading and after the injection nozzle just before the injection into the mold. Figure 12 shows the typical fiber cross sections, (a) after kneading and (b) after injection nozzle. As shown in the figures, the small compression around the fiber surface was found after the kneading, while the considerable compression was found after the injection nozzle. Therefore, the fibers should be compressed in the cylinder before the compound was injected into the mold. However, the compression ratio in Figure 11(b) seems to be rather higher than that in Figure 12(b). This indicates that the injection pressure and high shear rate in the mold channel might contribute the fiber compression.

Figure 13 shows the relationship between compression ratio and volume fraction of the fibers. The compression ratios were calculated by eq. (8). The compression ratio (2.7–3.6) in the bagasse fiber was considerably higher than that (1.2–1.4) in the kenaf. This result quite agrees with the difference of the fiber structure shown in Figures 4(a) and (c). Moreover, the compression ratio increased with increase of the volume fraction in both fibers. The reason being not clear, however, may be attributed to the kneading and injection process. The higher volume fraction of fibers would increase the interference among fibers in those processes.

From above results, the compression ratio K was assumed to 1.4 for kenaf and 3.6 for bagasse. In Figure

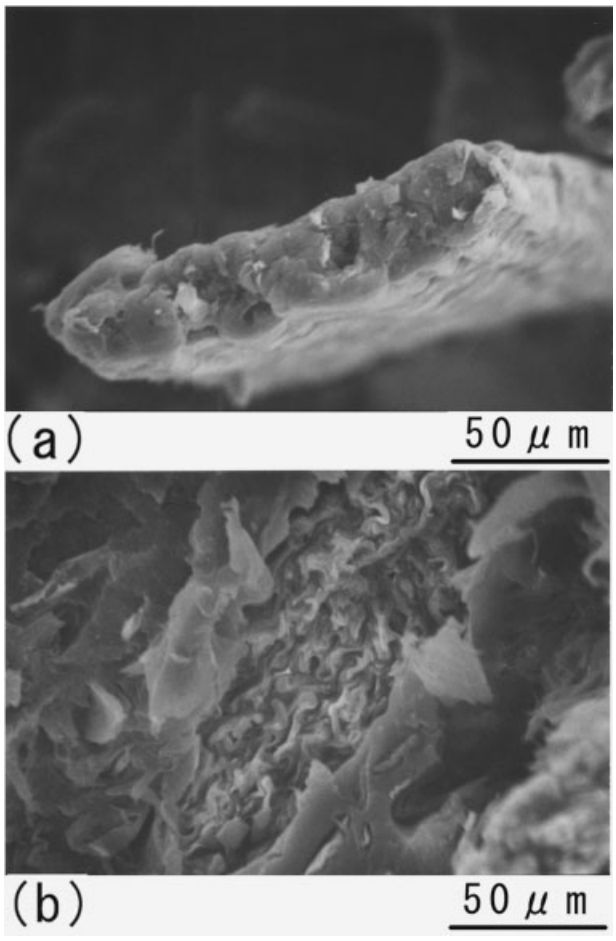

Figure 11 SEM microphotographs of the fiber cross section of the composite fracture surface after Charpy impact test, (a) kenaf (24 vol %) and (b) bagasse (26 vol %).

8, the lines were the calculation results by eq. (9). For reference, the calculation results without compression ratio K are shown. As shown in the figure, the calculation results were in good agreement with the experimental results. Therefore, it is concluded that the prediction model should incorporate the compression ratio for the prediction of the flexural modulus of natural fiber composites.

CONCLUSIONS

The flexural modulus of the natural fiber-reinforced composites by an injection molding was examined both in experimental and numerical calculation. The following conclusions were obtained.

The big scatter in the Young's modulus of kenaf and bagasse fiber was found. The fiber with high Young's modulus was more compressed than that with low Young's modulus. Both kenaf and bagasse have been chopped mechanically, and some of the fibers have been compressed before tensile test. Thus, the dense structure increases the Young's modulus of the natural fiber.

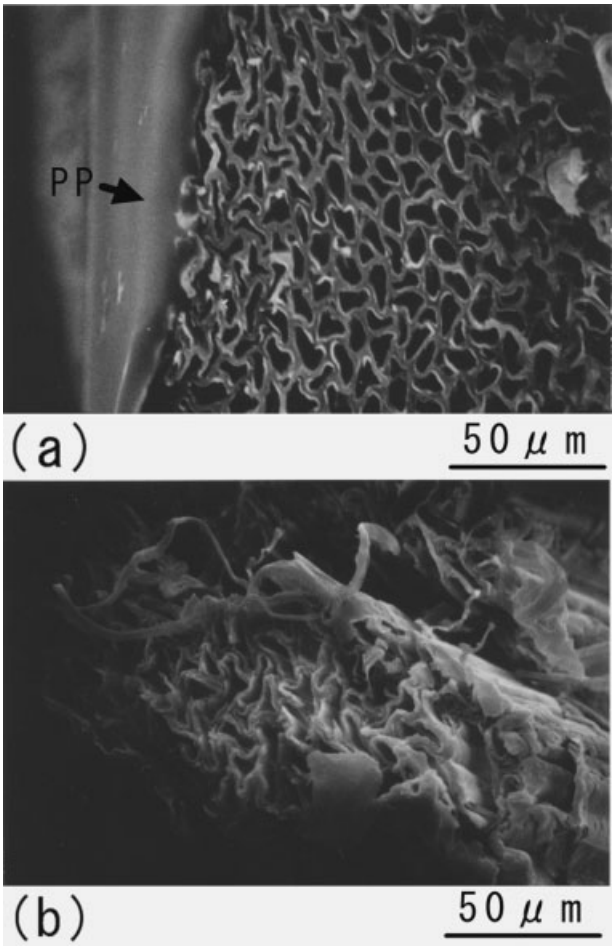

Figure 12 SEM microphotographs of the fiber cross section of the fracture surface, (a) after kneading process and (b) after injection nozzle.

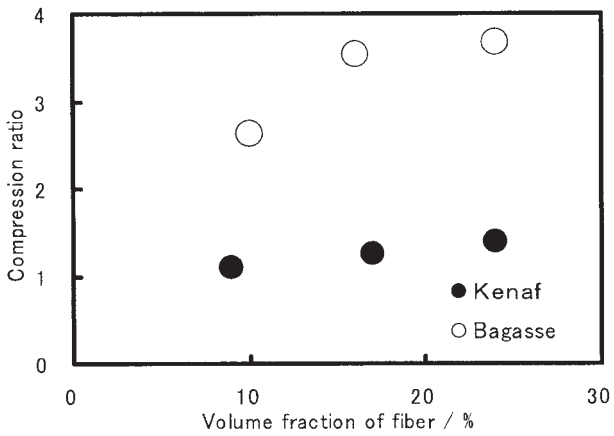

Figure 13 Relationship between compression ratio and volume fraction of composites.

In both fibers, the fiber orientation and length of the composites were similar. The distribution function of the fiber orientation in the composites was determined to be a triangular function.

The compression ratios in the composites were 1.2–1.4 for kenaf and 2.7–3.6 for bagasse. This difference was attributed to the cross section structures. Using these compression ratios, the flexural modulus was predicted by Cox's model that incorporated the effect of fiber compression. The predicted flexural modulus was in good agreement with the experimental. Moreover, the flexural modulus of the composites increased with the increase of the volume fraction of fibers.

References

1. Nishino, T; Hirao, K.; Kotera, M.; Nakamae, K.; Inagaki, H. Compos Sci Technol 2003, 63, 1281.
2. Karnani, R.; Krishnan, M.; Narayan, R. Polym Eng Sci 1997, 37, 476.
3. Karmaker, A. C.; Youngquist, J. A. J Appl Polym Sci 1996, 62, 1147.
4. Cichocki, F. R., Jr.; Thomason, J. L. Compos Sci Technol 2002, 62, 669.
5. Gowda, T. M.; Naidu, A. C. B.; Chhaya, R. Compos A 1999, 30, 277.
6. Ray, D.; Sarkar, B. K.; Rana, A. K.; Bose, N. R. Compos A 2001, 32, 119.
7. Gassan, J. Compos A 33, 369, 2002.
8. Wollerdorfer, M.; Bader, H. Ind Crop Prod 1998, 8, 105.
9. Keller, A. Compos Sci Technol 2003, 63, 1307.
10. Eichhorn, S. J.; Young, R. J. Compos Sci Technol 2004, 64, 767.
11. Hererra-Franco, P. J.; Valdez Gonzalez, A. Compos A 2004, 35, 339.
12. de Sousa, M. V.; Monteiro, S. N.; d'Almeida, J. R. M. Polym Test 2004, 23, 253.
13. Stael, G. C.; Tavares, M. I. B.; Almeida, J. R. M. Polym Test 2001, 20, 869.
14. Aziz, S. H.; Ansell, M. P. Compos Sci Technol 2004, 64, 1219.
15. Cox, H. L. Brit J Appl Phys 1952, 55, 72.
16. Hull, D. An Introduction to Composites Materials. Cambridge University Press: UK 1982.
17. Fukuda, H.; Chou, T. W. J Mater Sci 1982, 17, 1003.
18. Shibata, S.; Cao, Y.; Fukumoto, I. Polym Compos 2005, 26, 689.